Journal of Fluorescence, Vol. 12, Nos. 3/4, December 2002 (© 2002)

Fluorescence Probing of Cell Membranes with Azacrown Substituted Ketocyanine Dyes

A. O. Doroshenko,[1,3] L. B. Sychevskaya,[1] A. V. Grygorovych,[1] and V. G. Pivovarenko[2]

Received April 10, 2002; revised June 26, 2002; accepted June 27, 2002

The three dyes with similar fluorescence properties but different lipophility—azacrown- and dimethylamino-substituted ketocyanines—are proposed as probes for the studies of biomembrane structure and dynamics. Their attractive feature is an extremely strong solvatofluorochromism, covering the range from 470 to 650 nm. Two photophysical mechanisms are responsible for these features, the general polarity effect associated with substantial increase of the probe dipole moment on electronic excitation and the excited-state stabilization due to hydrogen bonding to the central carbonyl groups. On the binding of these probes with erythrocyte membranes, three components in fluorescence spectra are resolved. They are attributed to probe molecules bound in two discrete types of binding sites inside the membrane: *hydrophilic polar sites*, in which carbonyl groups of the probes molecules are hydrogenbonded with hydrogen donor surrounding, and *hydrophobic nonpolar sites*. The third component present in the emission spectra was attributed to the unbound probe in the near-membrane aqueous phase. Our results suggest that such a complex response of the probes is sensitive to the dynamics of hydration of the membrane interior, and this feature can be easily studied in simple ratiometric measurements. Among three studied compounds containing two crown-, two dimethylamino-, or both crown- and diethylamino- substituents, the latter proves to be most prospective in biomembrane research. This probe was tested in monitoring the phase transition of human erythrocyte membrane.

KEY WORDS: Fluorescent probes; ketocyanines; hydrogen bonding; protolytic interactions; erythrocytes; biomembranes; lipid bilayer phase transitions.

INTRODUCTION

Fluorescence techniques are very popular in various fields of molecular and cellular biology. Their advantages are high sensitivity, relative simplicity in methodology, and convenience in forming the image in cytological and cellular studies. The latter is largely due to the possibility of applying the probes with highly selective binding to cellular organelles, substructures, and biomembranes. Widening the arsenal of molecular probes, potentially available for investigating the structural, dynamic, and electrostatic properties of biological membranes, can be useful for understanding the complicated mechanisms of their functioning [1–3]. Promising in this respect are ketocyanine dyes and their azacrown-substituted derivatives, which possess a number of important features—a relatively high molar absorption, over 50 000 l/(mole·cm), reasonably high fluorescence quantum yields; and, most important—dramatic solvatochromic effect displayed both in absorption and fluorescence [4–5]. The solvent-dependent shifts in their fluorescence spectra may cover nearly the whole range of visible spectrum, from

[1] Institute for Chemistry at Kharkov V.N. Karazin National University, 4 Svobody sqr., 61077 Kharkov, Ukraine.
[2] Kyiv National Taras Shevchenko University, 64 Volodymyrska str., 01033 Kyiv, Ukraine
[3] To whom correspondence should be addressed. Tel.: +38 0572 45 73 35. Fax: +38 0572 45 71 30. e-mail: andrey.o.doroshenko@univer.kharkov.ua

1053-0509/02/1200-0455/0

blue-green to red [8–14]. Introduction of azacrown substituents can modulate the probe solubility and membrane-binding properties. In addition, these substituted probes can chelate alkali and alkali earth cations, which offers prospects for studying the binding of ions on the surface of biological membranes [4–7].

The formulas of crown- and dialkylamino-substituted ketocyanines, which are the object of our work, are presented below. Here **I** is 1,3-*bis*-[4-(*N*-aza-15-crown-5)-benzylidene]-cyclopentanone-2; **II** is 1-[4-(*N*-aza-15-crown-5)-benzylidene],3-[4-*N*,*N*-diethylamino-benzylidene]-cyclopentanone-2 and, III is 1,3-*bis*-[4-*N*,*N*-diethylamino-benzylidene]-cyclopentanone-2:

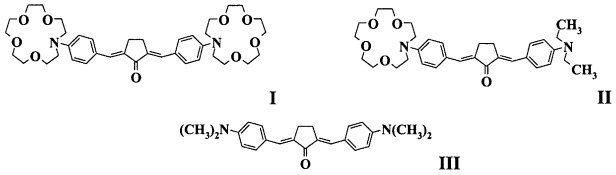

I II III

MATERIALS AND METHODS

Erythrocyte membranes free from hemoglobin (the so called "erythrocyte ghosts") were isolated according to common technique [15]. Protein concentration was studied by the Lowry method [16]. In our studies of probe binding, the membrane suspensions in 0.29 M aqueous sucrose solution were prepared with a constant protein concentration of 0.5 mg/mL ($6 \cdot 10^{-13}$g of proteins and $5 \cdot 10^{-13}$g of lipids in the membrane of a single erythrocyte).

The synthesis of mono- and *bis*-azacrown-substituted probes of the ketocyanine class (**I** and **II**) and also of model dimethylamino derivative (**III**) is described elsewhere [4,6,7]. Protonation of dialkylamino groups of the studied probes take place at pH 2–3 [4,5]; thus we consider our compounds in aqueous sucrose solutions (pH 5.5–6.5) and at their sorption into cell membranes to be in their unprotonated form. The same conclusion also could be made concerning their interaction with metal ions present in the near-membrane layers. Complexation of the dyes **I** and **II** by their azacrown moieties with alkali earth metal cations in acetonitrile takes place at concentrations of 0.01 M and higher [6]. Effectivity of complexation with alkali metals is much lower. We expect that the concentration of the residual metal ions in the cell membrane surrounding is lower in our experiments. Moreover, ejection of metal ions out of the azacrown cavity of azacrowned complexes at electronic excitation [17,18] compensates the effect of complexation onto their fluorescence properties and makes the latter practically the same as those for the corresponding non-complexed compounds [4,6]. Thus, possible interaction with metal ions and protons must not significantly affect the fluorescent properties of the probes **I–III** at their binding with cell membranes.

Electronic absorption spectra were measured on a Hitachi U3210 spectrophotometer. Spectrofluorimetric studies were conducted on Hitachi F4010 spectrofluorimeter in the standard 1-cm quartz cells in a thermostatically controlled cell holder at 25°C. No absorption of the studied dyes on the quartz surface was determined at our experiments with water sucrose solutions both with and without cell membranes suspension. Fluorescence spectra were presented in energy-proportional wavenumber scale (the intensity was expressed in a number of quanta per unit wavenumber range). In all our biological experiments **I–III** fluorescence was excited at 460 nm. Fluorescence quantum yields (φ_f) in homogeneous organic solvents were calculated in respect to solution of quinine bisulfate in 0.5 M aqueous sulfuric acid ($\varphi_f = 0.546$ [19], $\lambda^* = 380$ nm).

Numerical smoothing of the measured emission spectra (which was always made in order to minimize the experimental noise) was conducted according to Savitzki and Golay [20]. In some necessary cases numerical differentiation was made by the same method.

Mathematical separation of individual bands in fluorescence spectra was performed by the computer program specially developed in our research group, which uses iterational non-linear least squares method based on the Fletcher-Powell algorithm. The shapes of individual emission bands were approximated by log-normal function [21], which in contrast to usually applied Gauss or Lorentz functions accounts for the natural asymmetry of spectral band [Eq. (1)]. Below ν_{max}—position of the band maximum (cm^{-1}); I_{max}—intensity of the band in its maximum; H—half-width (cm^{-1}), the width of the band at the half of its intensity; ρ—asymmetry parameter. *A*, *B*, *C*—internal parameters, introduced to simplify the presentation of Eq. (1). For fluorescence bands $0 < \rho < 1$, and usually ρ values are greater than 0.5. In contrast, absorption bands are usually characterized by $\rho > 1$. Function $I(\nu)$ does not exist at $\nu > A$ for fluorescence spectra and at $\nu < A$ for absorption spectra. The absorption/emission intensity for these spectral regions was considered as equal to zero.

$$I(\nu) = I_{max} \cdot \frac{B}{\nu - A} \cdot \exp\left(- \frac{C^2 + \ln^2\left(\frac{\nu - A}{B}\right)}{2C} \right)$$

$$A = \nu_{max} - \frac{\rho \cdot H}{\rho^2 - 1}$$

$$B = \frac{\rho \cdot H}{\rho^2 - 1} \cdot \exp(C) \qquad (1)$$

$$C = \frac{\ln^2(\rho)}{2 \ln 2}$$

Parameters of log-normal functions (position of the maximum, ν_{max}, half-width H, and asymmetry ρ) were fitted by iteration procedure of non-linear least-squares method up to assessment of the maximal correspondence between the experimental and simulated spectra. Band intensities at their maxima, I_{max}, were determined by solution of the so-called "over-determined" system of linear equations by the linear least squares method. For the account of fluorescence emission of the probe molecules distributed in the aqueous phase, the experimentally determined emission spectra in the aqueous sucrose solution (of the approximately the same initial concentration of the probe) were introduced additionally into an iteration procedure in their numerical representation. Thus, for deconvolution of our experimental spectra we had to vary in the non-linear least squares scheme only six parameters, which determine the shape of two emission bands, rather than calculate intensities of three bands by the direct linear method (both these types of calculation were included into the same computer program). Variation of the emission bands shape parameters during all our experiments do not exceed a band maxima of 2–3%, band half-width of 7–9%, and asymmetry of 3–5%.

For estimation of the number of every elucidated type of binding sites for the probe on the membrane and of the corresponding binding constants the following approach was used. If we add sequentially small amounts (10 μL each) of relatively concentrated ethanolic solution of fluorescent probe to the cell suspension (2 mL of 0.29 M aqueous sucrose + 0.1 mL of initial membrane suspension, thus total amount of added ethanol at the highest concentrations did not exceeded 10–12%$_{vol}$), the probe would bind to the appropriate sorption zones and change its emission properties depending on the interaction with its nearest molecular surrounding. Addition of alcohol might cause the lipid bilayer interdigitation [22,23], which could change dramatically the biophysical properties of cell membrane. For some synthetic phospholipids, interdigitation happens at addition of 0.8–0.9M ethyl alcohol [24]; for erythrocyte membranes the ethanol-induced damages were detected at ethanol concentrations near 2.2 M [25]. In our case this effect seems to have minor influence because of two considerations: first, most of our quantitative treatment of experimental data was made for the concentrations of added ethanol below 1 M, for which interdigitation is still not important; second, no characteristic sigmoid inflections, which must indicate the changes in the erythrocyte membranes structure induced by alcohol, were observed on the concentrational curves of the probes **I–III**. However, we could not exclude to the end the effect of interdigitation of the erythrocyte lipid bilayer onto the studied ketocyanines fluorescence response at the highest amounts of the added ethanolic solutions.

So far as we assume the binding of our probes to two different binding sites on the membrane (see discussion below), we have to take into account two following equilibria:

$$L + M_1 \leftrightarrow (L \cdot M)_1 \quad L + M_2 \leftrightarrow (L \cdot M)_2$$

Here L is the equilibrium concentration of the unbound probe, M_1 and M_2 are the concentration of free binding sites on membrane, and $L{\cdot}M_1$ and $L{\cdot}M_2$ are the concentration of the probe molecules bound to membrane at the binding sites M_1 and M_2. To use the fluorescence data for estimation of binding constants we have to assume the concentration of free binding sites to be the difference in concentration of the probe in each binding site at conditions of their saturation by the added probe: $M_1 = LM_1^{max} - LM_1$ and $M_2 = LM_2^{max} - LM_2 \cdot LM_1^{max}$, LM_2^{max} mean the maximal reachable contents of the probes in both binding sites; these values could be approximately evaluated from the saturation points on the concentrational plots, presented on Fig. 3. Binding constants could be estimated by the following equations (further assuming the probe concentration to be proportional to its fluorescence response $c_{probe} \sim I_f/(\varphi_f \varepsilon_\lambda^*)$:

$$K_1 = \frac{[LM_1]}{[L] \cdot [M_1]} = \frac{[LM_1]}{[L] \cdot [LM_1^{max} - LM_1]}$$
$$K_2 = \frac{[LM_2]}{[L] \cdot [M_2]} = \frac{[LM_2]}{[L] \cdot [LM_2^{max} - LM_2]} \qquad (2)$$

To recalculate fluorescence intensities into concentrations the quantum yields (φ_f) and molar extinctions of the probes at the excitation wavelength (ε_λ^*) must be determined. The latter parameters were roughly estimated for the model conditions, for solvents possessing the polar properties close to those of the given binding sites (toluene and isopropyl alcohol, see discussion below). Thus, a total amount of the added probe, $\mathbf{L}_0$, redistributes between two types of binding sites and the aqueous phase: $\mathbf{L}_0 = L + L \cdot M_1 + L \cdot M_2$. Taking into account that at low probe concentrations the fluorescence intensity is proportional to molar concentration, molar extinction at the excitation wavelength, and quantum yield of the fluo-

rescent compound, $\mathbf{I}_f \sim c_M \cdot \varphi_f \varepsilon^*$, one can write: $L_0 = \alpha \cdot (\mathbf{I}_{aq}/\varphi_{aq}/\varepsilon^*_{aq} + \mathbf{I}_1/\varphi_1/\varepsilon_1^* + \mathbf{I}_2/\varphi_2/\varepsilon^*_2)$. Here α is the instrumental constant, which is necessary to convert fluorescence intensity into concentration. The latter can be determined for the concentrational ranges of the probes that were applied in our experiments, in which the α value remains unchanged within the experimental error (roughly $\pm$ 10–25%). Finally, the equations for binding constants (2) can be presented in the following way:

$$K_1 = \frac{I_1}{\alpha \cdot I_{aq}/\varphi_{aq}/\varepsilon_{aq} \cdot (I_1^{\max} - I_1)} \qquad K_2 = \frac{I_2}{\alpha \cdot I_{aq}/\varphi_{aq}/\varepsilon_{aq} \cdot (I_2^{\max} - I_2)} \tag{3}$$

The number of binding sites could be estimated roughly from the maximal values of fluorescence intensities of the probe, that are reached at saturation of the correspondent binding sites:

$$N_1 = \alpha \cdot \mathbf{I}_1^{max}/\varphi_1/\varepsilon_1^* \quad N_2 = \alpha \cdot \mathbf{I}_2^{max}/\varphi_2/\varepsilon_2^* \tag{4}$$

Concentration-dependent quenching of the probe fluorescence, inner-filter and reabsorption effects [26], and the effect of ethanol at its highest contents onto the erythrocyte membrane structure [22–25] could result in distortion of the results, obtained by the above presented scheme. Therefore here we would like to emphasize once more that the determination of binding constants was conducted at the lowest available concentrations of the added probes ($1 \div 2 \cdot 10^{-6}$ M for **I**, $3 \div 7 \cdot 10^{-6}$ M for **II**, $6 \cdot 10^{-7}$ M for III).

RESULTS AND DISCUSSION

Biological cell membranes are rather complex and inhomogeneous by their internal construction. The erythrocyte (red blood cells, RBC) membrane, which was selected for study in this paper, could be approximately classified as consisting of several zones different by their polarity and hydration extent: the zone of lipidic long-chain fatty acid tails, esteric residues zone (both acylglycerol and phosphate), and the zone of glycoproteins, a highly hydrated layer at the surface of the biomembrane [27]. The first two zones belong to the inner lipid layers of the bulk of the membrane and are of nearly 30 Å in width. The other is the marginal zone between the lipid membrane and surrounding water phase, and its width might be roughly estimated as ~100 Å [27].

Fluorescent probes of the ketocyanine series (**I–III**) possess spectral properties that allow reliable evaluation of the polarity and total hydrogen bonding ability of their surrounding. Having practically the same chromophoric unit, these molecules are close one to another by their spectral parameters. Our study of their spectral properties in pure and mixed solvents [5,28] has shown they could be rather good models for the probes in biological systems. Basing on the above-mentioned results, we could expect the positions of the fluorescence maxima of the probes at their location in the low-polar zone of the lipidic hydrocarbon chains not to exceed 500 nm, such as in toluene-hexane mixtures. At location of the probes in close contact with the esteric glycerol or phosphoric acid residues, their emission must be shifted toward 530–560 nm, such as in the toluene-triacetin mixed-solvent system. When water molecules appear in such a zone, no considerable change in the fluorescence spectra is expected, rather, only a slight increase in the emission intensity and further batofluoric shift to 580 nm (model solvent system of toluene-alcohol mixtures with alcohol contents below 10 mole/L; pure isopropyl alcohol solution displays nearly the same emission characteristics). At increasing of protic component contents from 10 to 55 mole/L (such as in toluene-methanol and acetone-water mixtures), we registered considerable decrease in our probes emission intensity. The possible reasons for such behavior have been the subject of intensive study during recent years [9,12,13,29]. However, no widely accepted clarification of this behavior has been elaborated. The noticeable red shift in emission (to 660 nm in water sucrose) is observed for probes in highly proton donating surroundings.

So, the dramatic dependence of the studied ketocyanine probes' spectral properties allows us, from one side, to elucidate the predominant location of the probe molecules inside the membrane, and, from another side, to monitor the changes in the nature of the closest surrounding of our probes at definite changes in the structure of the membrane caused by several "external" factors. Moreover, usage of the probes with close spectral parameters but different lipophility allows us to collect additional information concerning the properties of the membrane zones, which differ by their polarity and hydration extent.

For the application of our probes in biomembrane studies we need primarily to establish the number and affinity of binding sites and thus to respond to the question of how the probes interact with the membranes. Our preliminary study has shown the very weak interaction of our probes with proteins: practically no difference in fluorescence intensity, position, and shape of **I–III** emission spectra was found for water solutions containing human serum albumin in respect to corresponding water sucrose solutions. Contrary to the above observations, significant improvement of fluorescence ability in lipo-

somic surroundings was detected for **I–III**, where their emission intensity increased 1–2 orders of magnitude. Thus, we consider our fluorescent dyes as predominantly lipid probes and practically insensitive to proteins.

From the analysis of structural formula of compounds **I–III**, these probes should differ substantially in their lipophility. The empirical estimate of a widely employed lipophility parameter, the logarithm of the distribution constant in the system octanol-1—water (*logP*), determined by the additive scheme [30,31] resulted in the following data: *logP* = 2.99 for **I**, 5.43 for **II**, and 5.74 for **III**. Thus, based on the obtained *logP* values, we expect all our probes will readily penetrate into lipid membrane; however, their location will be different sites of membrane.

The fluorescence spectra obtained on sequential addition of the small amounts of the probes dissolved in ethanol to a suspension of erythrocyte membranes in 0.29 M aqueous sucrose solution are presented in Fig. 1. All the emission spectra are significantly broadened in comparison with that measured in pure organic solvents or in their mixtures, and occupy nearly the whole visible region. They present a complex emission of the probe located in multiple binding sites of different polarity inside the membrane, and include emission from the near-membrane water phase, as well. The shape of the spectral curves and positions of the maxima differ for every studied probe. However, the obtained data show that overwhelming quantities of the probes penetrate into the membrane. This follows from the near 10 times higher emission intensity of the probes in the presence of membranes than in their absence. A definite exception is the less lipophilic probe **I**, which at higher concentrations than $2.5 \cdot 10^{-6}$ M (spectrum 11 at Fig. 1a) distributes preferably into the water phase. Emission intensity of the probe **I** in membrane reaches saturation at these concentrations, as can be seen from the data of Fig. 1 (and more clearly in Fig. 3).

Let us start our consideration of the interaction of **I–III** dyes with biomembranes from the most lipophilic among them, probe **III**. For this compound, two satisfactory resolved bands seem to be present in its fluorescence spectra. An example of deconvolution of the total fluorescence spectrum of probe **III** into individual emission components is presented in Fig. 2c (together with the analogous deconvolution examples for the other probes). Positions of two main emission bands are close to the corresponding fluorescence spectra in toluene and isopropyl alcohol (Table 1). The intensity of emission of **III** from the aqueous phase is very low and increases only at higher contents of the added probe.

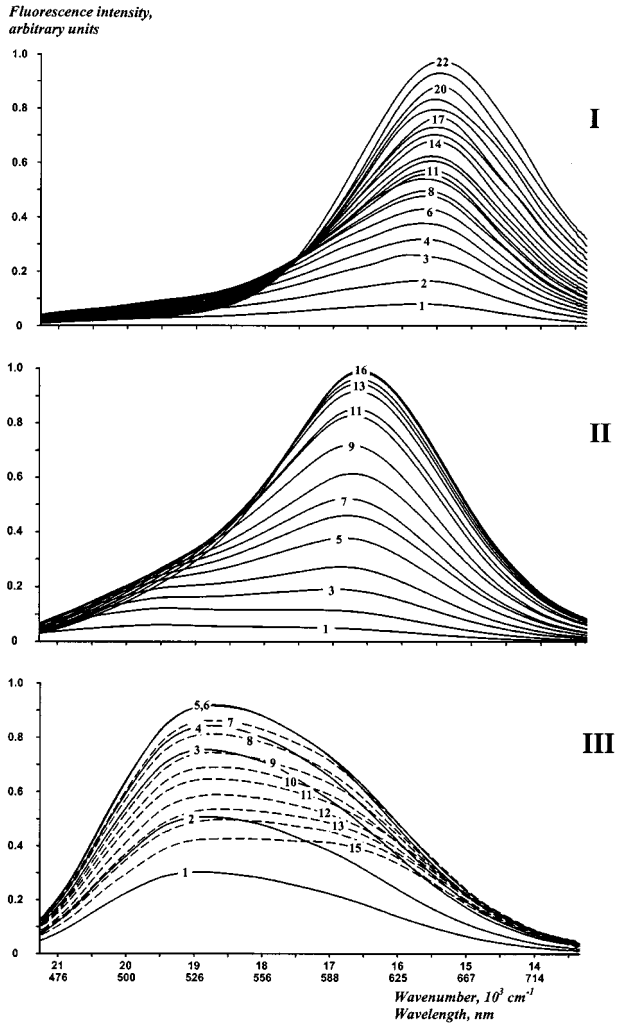

Fig. 1. Fluorescence spectra of the probes **I–III** at their binding with erythrocyte membranes. Concentrations of the probes added to suspension of membranes: **I**: 1 = $2.38 \cdot 10^{-7}$, 2 = $4.73 \cdot 10^{-7}$, 3 = $7.06 \cdot 10^{-7}$, 4 = $9.37 \cdot 10^{-7}$, 5 = $1.16 \cdot 10^{-6}$, *6 = 1.39 · 10*$^{-6}$, 7 = $1.61 \cdot 10^{-6}$, 8 = $1.84 \cdot 10^{-6}$, 9 = $2.06 \cdot 10^{-6}$, 10 = $2.27 \cdot 10^{-6}$, 11 = $2.49 \cdot 10^{-6}$, 12 = $2.7 \cdot 10^{-6}$, 13 = $2.91 \cdot 10^{-6}$, 14 = $3.12 \cdot 10^{-6}$, 15 = $3.53 \cdot 10^{-6}$, 16 = $3.74 \cdot 10^{-6}$, 17 = $3.94 \cdot 10^{-6}$, 18 = $4.34 \cdot 10^{-6}$, 19 = $4.53 \cdot 10^{-6}$, 20 = $4.92 \cdot 10^{-6}$, 21 = $5.48 \cdot 10^{-6}$, 22 = $6.03 \cdot 10^{-6}$ Mole/L; **II**: 1 = $4.9 \cdot 10^{-7}$, 2 = $9.73 \cdot 10^{-7}$, 3 = $1.45 \cdot 10^{-6}$, 4 = $1.92 \cdot 10^{-6}$, 5 = $2.4 \cdot 10^{-6}$, 6 = $2.96 \cdot 10^{-6}$, *7 = 3.32 · 10*$^{-6}$, 8 = $3.78 \cdot 10^{-6}$, 9 = $4.23 \cdot 10^{-6}$, 10 = $4.67 \cdot 10^{-6}$, 11 = $5.12 \cdot 10^{-6}$, 12 = $6.0 \cdot 10^{-6}$, 13 = $6.42 \cdot 10^{-6}$, 14 = $6.85 \cdot 10^{-6}$, 15 = $7.7 \cdot 10^{-6}$, 16 = $8.1 \cdot 10^{-6}$ Mole/L; **III**: 1 = $4.42 \cdot 10^{-8}$, 2 = $2.83 \cdot 10^{-7}$, 3 = $4.22 \cdot 10^{-7}$, 4 = $5.6 \cdot 10^{-7}$, 5 = $6.97 \cdot 10^{-7}$, 6 = $8.52 \cdot 10^{-7}$, 7 = $9.66 \cdot 10^{-7}$, 8 = $1.1 \cdot 10^{-6}$, 9 = $1.23 \cdot 10^{-6}$, *10 = 1.36 · 10*$^{-6}$, 11 = $1.49 \cdot 10^{-6}$, 12 = $1.62 \cdot 10^{-6}$, 13 = $1.74 \cdot 10^{-6}$, 14 = $1.87 \cdot 10^{-6}$, 15 = $1.99 \cdot 10^{-6}$ Mole/L. Spectra for this compound, in which intensity decreases with the increase of the probe concentration, presented in broken lines.

Table I. Fluorescence Parameters of the Probes **I-III** Bound to Erythrocyte Membranes and Correspondent Data for the Prototype Model Solvents (Positions of Emission Bands Maxima, Quantum Yields, and Extinctions on the Excitation Wavelength, 460 nm), Which Were Used for Estimation of Their Binding Ability With the RBC Membrane

Compound	Emission of the probes absorbed on erythrocyte membranes ν_{max}, cm^{-1} (λ_{max}, nm)		Prototype solvent ν^f_{max}, cm^{-1} (λ_{max}, nm)		φf	ε^*_{460} $1 \cdot mole^{-1} \cdot cm^{-1}$
I	Non-polar zone (1)	19760 (506)	Toluene	19260 (519)	0.18	77000
	Polar zone (2)	16540 (605)	Isopropyl alcohol	16540 (605)	0.45	64000
	Water Phase	15320 (652)	Aqueous sucrose	15320 (652)	0.015	62000
II	Non-polar zone (1)	19080 (524)	Toluene	19240 (520)	0.18	68200
	Polar zone (2)	16700 (599)	Isopropyl alcohol	16900 (592)	0.38	55300
	Water Phase	15640 (639)	Aqueous sucrose	15640 (639)	0.010	47500
III	Non-polar zone (1)	19340 (517)	Toluene	19340 (517)	0.11	58900
	Polar zone (2)	17040 (587)	Isopropyl alcohol	16980 (589)	0.26	59000
	Water Phase	15820 (632)	Aqueous sucrose	15820 (632)	0.011	53400

In our opinion, this suggests the presence of two types of binding sites, which are distinguished by interaction of probe molecules with the environment. These sites may differ in polarity and ability to form hydrogen bonds with probe carbonyl groups [28]. Thus, the short-wavelength band (517 nm) probably corresponds to the probe buried more deeply into the hydrophobic inner-layers of the membrane, while the long-wavelength band (587 nm) may correspond to the probe molecules localized in more polar membrane areas. Besides higher polarity, higher hydration and/or the presence of other donors of hydrogen bond probably characterizes the last type of binding sites.

The dependence of relative fluorescence intensity of probe **III** on concentration reaches saturation at concentrations near $1 \cdot 10^{-6}$ M and then decreases noticeably, probably as a result of an efficient concentrational fluorescence quenching in the binding sites at the conditions of their saturation (Fig. 3c). This must not be due to the added alcohol effect on the membrane structure because total alcohol contents in the membrane suspension is relatively low in the discussed case. Because compound **III** has the highest lipophility parameter of the probes studied, this suggests that the probe surrounding is mostly hydrophobic. Also the binding constants (estimated with the help of data for model solvents; see Table 1) in this case are much higher then for the other studied compounds. Application of the procedure, described in the *Materials and Methods* section to the emission data of **III** on erythrocyte membranes results in the following binding constant values for non-polar and polar hydrated sites: $K_2^{III} = (2.8 \pm 1.1) \cdot 10^8$ and $K_2^{III} = (1.6 \pm 0.5) \cdot 10^8$ $mole^{-8}$. Also the number of these two types of binding sites could be roughly estimated for **III** as $N_1^{III} = 600$ and $N_2^{III} = 230$ nanomole/mg of lipids correspondingly. Highest ΔG values ($\Delta G = -RT \cdot ln\mathbf{K}$) for the binding of **III** with erythrocyte membranes (~11 kcal/mole) in the studied series of ketocyanine probes also evidences about the mostly hydrophobic type of interaction of these probe and erythrocyte membrane in the discussed case [32]. Two other probes binding with RBC ghost membranes was characterized by ΔG ~7–9 kcal/mole.

The lipophility parameter of probe **II** is lower than that of probe **III**, because of highly hydrophilic azacrown moiety present in this molecule. The change in the character of the probe **II** binding is easily revealed by the difference in its fluorescence spectrum in the membrane suspension (see Fig. 1b) compared to that of probe **III**. In the case of **II** the necessity to account the emission of the unbound probe in the solution arises dramatically (Figs. 1b and 2b). As expected, the magnitude of this third component in the emission spectra of **II** on cell membrane linearly increases its intensity at the increase of total probe concentration. It becomes especially important, when the binding sites in the membrane become occupied, and the probe molecules are accumulated mainly in near-membrane aqueous sucrose solution.

The results of deconvolution of spectra **II** evidences also that there are two distinct types of binding sites in the membrane as well. The short-wavelength band (524 nm) corresponds by its position to fluorescence spectrum in low-polar medium, which is probably close by its polarity to toluene. The long-wavelength band (599 nm) corresponds to emission spectrum in relatively polar proton-donor medium because it is close to position of the spectrum in isopropyl alcohol. The intensity of the second band is higher, which might witness for preferential binding of probe **II** in more polar and hydrated areas of the RBC membrane. The estimated binding constant for the polar binding site, $K_2^{II} = (2.1 \pm 0.6) \cdot 10^5$ $mole^{-1}$ is

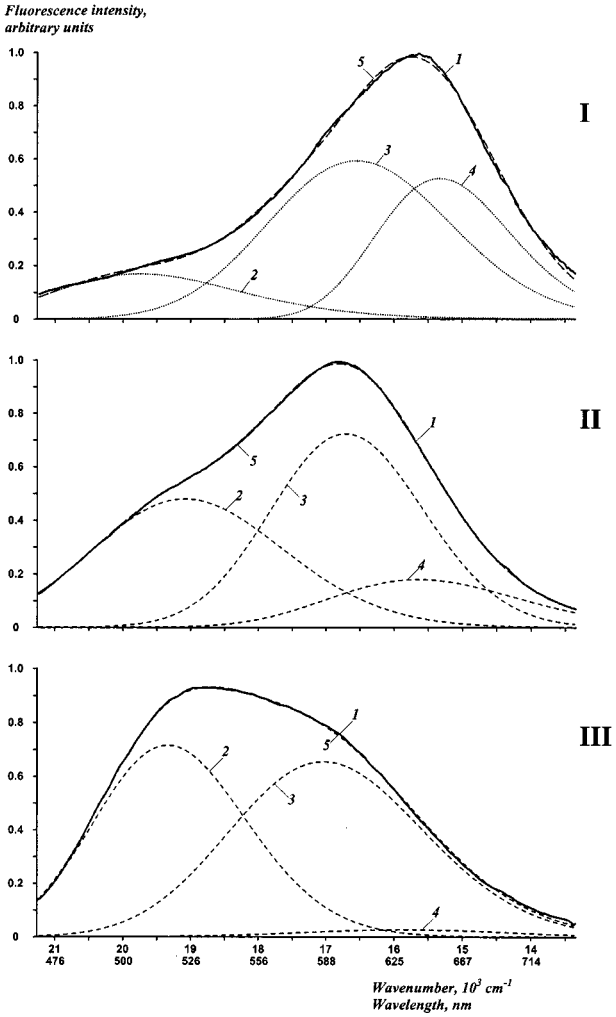

Fig. 2. Examples of mathematical deconvolution of fluorescence spectra of probes **I** ($1.39 \cdot 10^{-6}$ Mole/L, spectrum *6* in figure 3a), **II** ($3.32 \cdot 10^{-6}$ Mole/L, spectrum *7* in figure 3b), and **III** ($1.36 \cdot 10^{-6}$ Mole/L, spectrum *10* in figure 3c) at their binding with erythrocyte membrane (*1* = experimental spectrum, *2* = emission of probe, bonded to the non-polar binding site, *3* = emission of probe, bonded to the polar hydrated binding site, *4* = emission from aqueous phase, *5* = sum of the spectral curves 2, 3 and 4; normally they differ very little from the initial experimental spectra).

nearly 10 times lower in comparison to that of non-polar site, $K_1^{II} = (2.2 \pm 0.6) \cdot 10^6$ mole^{-1}. Thus the mentioned difference in the intensities of two emission bonds of **II** absorbed on membrane could be connected with the difference in the number of binding sites (N_1^{II} = 620 nanomole/mg of lipids for non-polar and N_2^{II} = 850 nanomole/mg of lipids for hydrated sites) and also in the significant increase of the unbounded probe content in the aqueous phase.

Analysis of the number of binding sites and association constants demonstrates that the interaction of the probe **II** with the polar part of the membrane is characterized by lowest K_2^{II} and highest N_2^{II} values within the studied series. A significant number of binding sites allow suggesting that the probe is located at the polar interface between the lipid bilayer and water. In view of strong asymmetry of this molecule and the presence in it of the well-distinguished hydrophilic and lipophilic parts, we can assume its orthogonal orientation toward the membrane surface with hydrophobic part immersed into membrane bilayer and the azacrown group exposed to aqueous medium. In this orientation the association with membrane is easier and the number of binding sites is greater. Relative contribution of these two types of binding sites may change as a result of action of different factors changing the membrane structure and internal dynamics. Thus, taking into account relatively higher emission intensity among the studied compounds, compound **II** appears to be a very promising membrane probe sensitive to the processes occurring on the membrane surface.

Probe **I** is the most hydrophilic of the studied compounds. Its fluorescence spectra witness that this probe binds preferentially with the biomembrane surface: the intensity of a low-wavelength emission band is much lower in comparison to the long-wavelength one (Fig. 1a–3a). However, because of its higher solubility in water, a significant amount of the probe added to the erythrocyte membrane suspension remains unbound (Fig. 3a). For probe **I**, similarly to the other probes, the short-wavelength component in the fluorescence spectrum (506 nm) is observed due to emission of probe molecules bound at hydrophobic binding sites, but at low intensity and only at low probe concentrations. On increase of the probe content, this component hides under the more intensive bond belonging to the probe bound to membrane surface, and, to a larger extent, to the probe distributed in aqueous phase as well. Numerical data, which characterizes this probe binding to membrane, are the following: $K_1^I = (4.0 \pm 1.5) \cdot 10^6$ mole^{-1}, N_1^I = 80 nm/mg of lipids; $K_2^I = (2.2 \pm 1.1) \cdot 10^6$ mole^{-1}, N_2^I = 100 nm/mg of lipids. Owing to the fact that compound **I** does not penetrate substantially inside membrane layers, it provides less promising prospects for use in the investigation of membrane properties and dynamics of intermembrane processes; however its use for investigation of membrane surface seems to have definite prospects.

To demonstrate the principle applicability of our probes to study the biomembrane structure and dynamics, we have attempted to monitor the phase transition inside the lipid bilayer of RBC membranes with the help of probe **II**. It is commonly accepted that biological membrane phospholipids, which form its lipid bilayer, could exist in two alternative conditions [33,34]: in *solid gel*

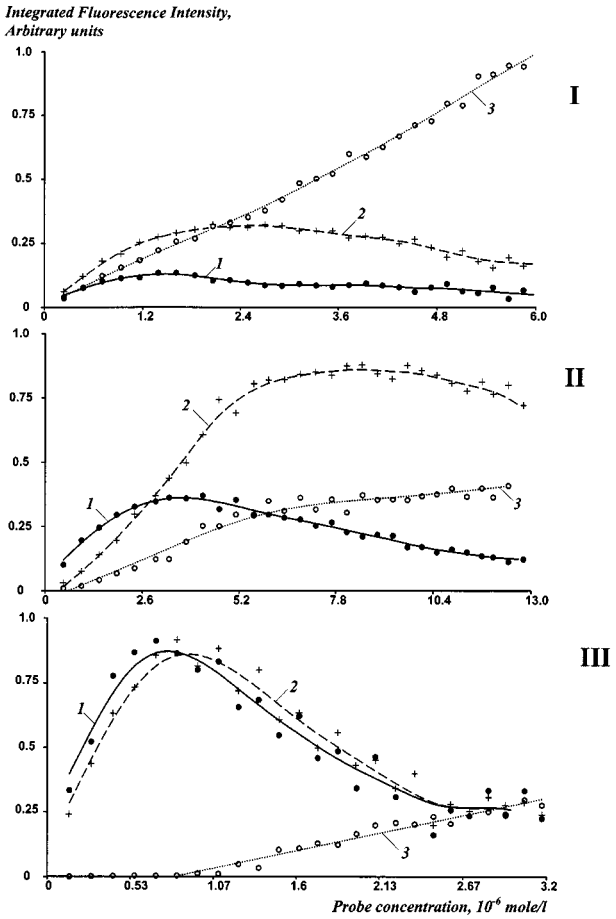

Fig. 3. Fluorescence of probes **I–III**, absorbed on erythrocyte membranes in respect to the total concentration of the added probe: *1* = emission from the non-polar binding site (solid circles), *2* = from the polar hydrated site (crosses), *3* = from the water sucrose phase (open circles). Curved lines were drawn through the experimental data points with the help of "smoothing spline" procedure.

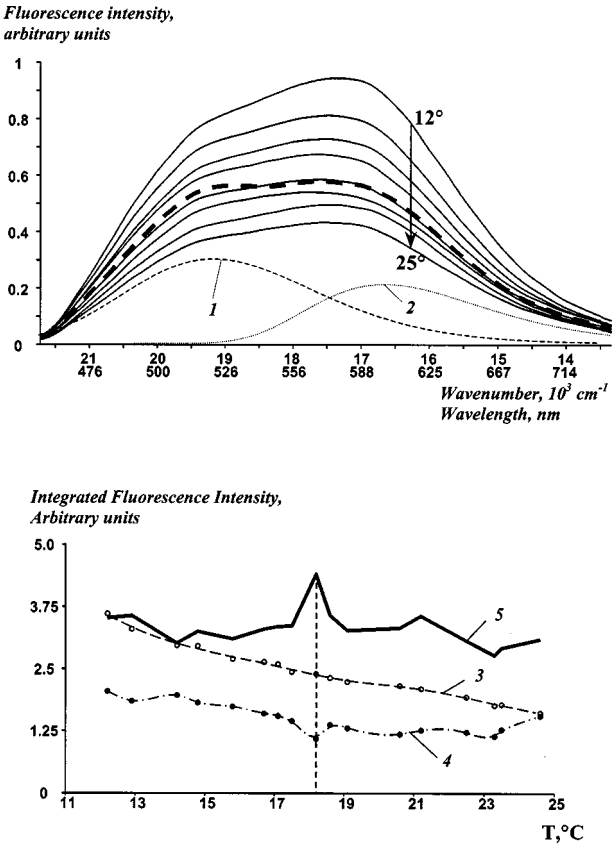

Fig. 4. Fluorescence of the probe **II** ($\sim 1 \cdot 10^{-6}$ Mole/L) absorbed into erythrocyte membrane in the temperature range 12–25°C (above) and the example of the spectrum deconvolution into its components for the temperature of 25°C (*1* = non-polar zone, λ_{max} 525 nm, *2* = polar hydrated zone, λ_{max} 600 nm; emission from the water phase was low, it is not shown). Plot of this probe integrated fluorescence intensity from the hydrophobic zone (*3*) and from the hydrated zone (*4*) together with their ratio (*5*, doubled) as a function of temperature (below). Sharp intensity ratio jump at the temperature of lipid bilayer phase transition is clearly seen at ~18°C.

phase and in *liquid crystalline* phase: The first is characterized by more rigid alignment of lipid hydrocarbon chains, whereas increased internal flexibility is typical to the other phase. Correspondingly, the solid gel phase exists at lower temperatures and the liquid crystalline phase at higher ones. Phase transition takes place in a small temperature range, which has been elucidated for human erythrocytes by several authors with various physical methods, between 16 and 20°C. Thus, the Raman spectroscopy data gave a value of 17°C [35]; the viscosity changes study, 18–19°C [36]; ^{31}P NMR data, 20°C [37]; positron annihilation, 16–18°C [38]; spin label study 18°C [39]; fluorescence probing utilizing the photodissociation of 1-naphthol 19°C [40].

The results of our temperature measurements are presented in Fig. 4. Temperature quenching of fluorescence with nearly the same efficiency was found for this probe absorbed both into the inner non-polar binding zone and into the closer to surface polar hydrated zone. However, in the last case the quenching efficiency had being somewhat accelerated at the temperature close to the expected phase transition. The latter circumstance was more clearly displayed, when intensity ratio $I_{non\text{-}polar}/I_{hydrated}$ is plotted against temperature. The jump in this ratio at 18°C was rather sharp; however, to our understanding, it exceeds the usual noise level. This is analogous to the "sharp jump" of fluorescence response and restoration of the initial signal level after passing the transition temperature in nearly the same narrow temperature range as was reported for studying the erythrocytic lipids phase transition with the use of 1-naphthol as fluo-

rescent probe [40]. Our results are also in rather good agreement with those reported by another authors cited above [35–39].

Probably, at phase rebuilding of the erythrocyte lipid bilayer, the penetration of water molecules into the near-surface esteric zone of the latter became more pronounced. This might result in the temporary acceleration of fluorescence quenching of the definite fraction of probe **II**, localized in this area of the membrane. No sharp disturbance in the smooth temperature-quenching plot for the probe in deeper non-polar zone was detected. After phase rebuilding is finished, the initial value for the discussed intensity ratio is restored.

Our observations allow us to conclude that the fluorescence intensity ratio measured for the ketocyanine probes absorbed into the cell membranes could be used as a sensitive indicator for the changes in biomembrane structure. This opens the possibility for creating analytical methods not only for monitoring the above described phase transitions, but also for the studying of any changes in membrane internal construction by the influence of various external damaging factors, such as X rays, laser irradiation, hazardous chemicals, etc.

CONCLUSIONS

Azacrown- and dimethylamino-substituted ketocyanines display themselves as prospective probes for biomembrane studies, because their fluorescence spectra are substantially dependent from the environment and vary in extremely broad ranges, from 470 to 650 nm. Moreover, in localized environments they may display satisfactory resolved discrete spectral bands. Our earlier results demonstrated that two mechanisms are involved in dramatic solvatochromic and solvatofluorochromic effects exhibited by these probes. One is the general polarity, associated with substantial increase of the probe dipole moments at electronic excitation. The other is an additional stabilization of the excited state due to formation of hydrogen bonds by the probe carbonyl group with proton-donor groups of the probe surroundings. For the first time in fluorescence biomembrane studies, in this report the discrete character of probe binding with erythrocyte membranes was demonstrated by resolving three satisfactory separated components of fluorescence emission of the probe. These components were attributed to the probe molecules bound to two discrete types of binding sites—polar hydrophilic and low-polar lipophilic ones, and also to unbound probe in aqueous phase. It is essential that for probes that differ significantly in their lipophility and membrane-binding properties, these discrete components are very similar, and the most marked difference is observed in their relative contribution to the total fluorescence response.

In the present study we were not able to give detailed characteristics to the discrete probe binding sites in erythrocyte membrane. It is highly probable that these sites differ by their access to the probes molecules by intercellular water. Depending upon the site they can penetrate or not penetrate, and whether they can bind or not bind with the carbonyl group of the probe, this probably the origin of discrete spectroscopically resolved forms of the ketocyanine probes bound to cell membrane. It is known that water is not an integral component of biological membranes; its penetration into membrane is dynamic, so our probes should be primarily tested for their sensitivity to dynamic properties of cell membranes and correlated with other parameters characterizing these properties, in particular, with membrane fluidity. It is essential that the studied probes offer a sensitive and convenient feature of their fluorescence response—ratiometric measurement at two separated wavelengths. Out of three studied probes, a mono-crown dibenzylidene-cyclopentanone derivative **II** is most promising because of its amphiphilic properties and the highest number of the binding sites on the cell membrane. The successful monitoring of the temperature-dependent phase transitions in the lipid bilayer of human erythrocyte membranes was conducted with the help of this probe.

ACKNOWLEDGMENTS

The reported work, during its starting period, was supported by INTAS-96 program (project 96-1225). The authors express their sincere gratitude to professors A. P. Demchenko (Ukraine/Turkey) and V. I. Dreval (Ukraine/Germany) for their interest in this work and valuable and helpful discussion of the results.

REFERENCES

1. Yu. A. Vladimirov, and G. E. Dobretsov (1980) *Fluorescent Probes in the Investigation of Biological Membranes.* Nauka, Moscow.
2. L. M. Loew (1988) *Spectroscopic Membrane Probes*. CRC Press, Deerfield Beach, FL.
3. J. M. G. Torres-Pereira, H. W. Wong Fong Sang, A. P. R. Theuvenet, and R. Kraayenhof (1984) Electric surface charge dynamics of chloroplast thylakoid membranes. Temperature dependence of electrokinetic potential and aminoacridine interaction. *Biochim. Biophys. Acta* **767**, 295–303.
4. A. O. Doroshenko, A. V. Grigorovich, E. A. Posokhov, V. G. Pivovarenko, and A. P. Demchenko (1999) *Bis*-azacrown derivative of di-benzilidene-cyclopentanone as alkali earth Ion chelating probe: spectroscopic properties, proton accepting ability and complex formation with Mg^{2+} and Ba^{2+} ions. *Molec. Eng.* **8**, 199–215.

5. A. O. Doroshenko, A. V. Grigorovich, E. A. Posokhov, V. G. Pivovarenko, and A. P. Demchenko (2000) Spectroscopic properties and proton accepting ability of N-alkyl derivatives of dibenzilidenecyclopentanone, prospective fluorescent probes for cell membrane investigation. *Funct. Mater.* **7**, 323–329.
6. A. O. Doroshenko, A. V. Grigorovich, E. A. Posokhov, V. G. Pivovarenko, A. P. Demchenko, and A. D. Sheiko (2001) Complex formation between azacrown derivatives of dibenzilidenecyclopentanone and alkali-earth metal ions. *Russ. Chem. Bull. Int. Educ.* **50**, 404–412.
7. N. Marcotte, S. Fery-Forgues, D. Lavabre, S. Marguet, and V. G. Pivovarenko (1999) Spectroscopic study of a symmetrical biscrown fluoroinophore of the diphenylpentadienone series. *J. Phys. Chem. A* **103**, 3163–3170.
8. C. Reichardt (1994) Solvatochromic dyes as solvent polarity indicators. *Chem. Rev.* **94**, 2319–2358.
9. V. V. Danilov, G. G. Dyadyusha, and A. A. Rykov (1984) The solvatochromism of ketocyanines and the formation of hydrogen bonds by the carbonyl group. *Russ. J. Phys. Chem. (Engl. Transl.)* **58**, 556–560.
10. N. B. Arzheukhova, V. V. Danilov, and V. S. Libov (1982) Absorption and fluorescence spectroscopic study of the solvatochromism of ketocyanines in liquid crystals. *Russ. J. Phys. Chem. (Engl. Transl.)* **56**, 1212–1215.
11. L. A. Shvedova, A. S. Tatikolov, Zh. A. Krasnaya, and V. A. Kuzmin (1990) Photochemistry of ketocyanine dye—polyenic bis-ω,ω′-amino ketones substituted in the polyene chain. *Bull. Acad. Sci. USSR Div. Chem. Sci. (Engl. Transl.)* **39**, 1369–1375.
12. M. V. Barnabas, A. Liu, A. D. Trifunac, V. V. Krongauz, and C. T. Chang (1992) Solvent effects on the photochemistry of a ketocyanine dye and its functional analogue, Miehler's Ketone. *J. Phys. Chem.* **96**, 212–217.
13. D. Banerjee, A. K. Laha, and S. Bagchi (1995) Solvent dependent absorption and fluorescence of ketocyanine dye in neat and binary mixed solvents. *Indian J. Chem.* **34**, 94–101.
14. D. Banerjee, P. K. Das, S. Mondal, S. Ghosh, and S. Bagchi (1996) Interaction of ketocyanine dyes with cationic, anionic and neutral micelles. *J. Photochem. Photobiol. A Chem.* **98**, 183–186.
15. Dodge, C. Mitchell, and D. Hanahan (1963) The preparation and chemical characteristics of hemoglobin-free ghosts of human erythrocytes. *Arch. Biochem. Biophys.* **100**, 119–130.
16. O. H. Lowry, N. J. Rosebrough, A. L. Farr, and R. J. Randall (1951) Protein measurement with the Folin phenol reagent. *J. Biol. Chem.* **193**, 265–279.
17. J. Bourson and B. Valeur (1989) Ion-responsive fluorescent compounds. 2. Cation-steered intramolecular charge transfer in a crowned merocyanine. *J. Phys. Chem.* **93**, 3871–3876.
18. M. M. Martin, P. Plaza, N. Dai Hung, Y. H. Meyer, J. Bourson, and B. Valeur (1993) Photoejection of cations from complexes with a crown-ether-linked merocyanine evidenced by ultrafast spectroscopy. *Chem. Phys. Lett.* **202**, 425–436.
19. W. A. Melhuish (1967) Quantum efficiencies of fluorescence of organic substances: effect of solvent and concentration of the fluorescent solute. *J. Phys. Chem.* **65**, 229–235.
20. A. Savitzky and M. J. E. Golay (1967) Smoothing and determination of data by simplified least squares procedures. *Anal. Chem.* **337**, 1627–1639.
21. D. B. Siano and D. E. Metzler (1969) Band Shapes of the Electronic Spectra of Complex Molecules. *J. Chem. Phys.* **51**, 1856–1861.
22. J. L. Slater, C. H. Huang (1988) Interdigitated bilayer membranes. *Progr. Lipid. Res.* **27**, 325–359.
23. N. E. Nagel, G. Cevc, S. Kirschner (1992) The mechanism of the solute induced chain interdigitation in phosphatidylcholine vesicules and characterization of the isotermal phase transitions by means of dynamic light scattering. *Biochim. Biophys. Acta* **1111**, 263–269.
24. E. S. Rowe (1983) Lipid chain length and temperature dependence of ethanol phosphatidylcholine interaction. *Biochemistry* **22**, 3299–3305.
25. I. B. Zavodink, T. P. Piletskaya, and I. I. Stepuro (1994) Kinetics of ethanol-induced hemolysis of human erythrocytes. *Biofizika (Russ.)* **39**, 1033–1039.
26. J. N. Miller (Ed.) (1981) *Standards in Fluorescence Spectroscopy* Chapman and Hall Ltd., London, New York, pp. 27–43.
27. R. B. Gennis (1989) *Biomembranes: Molecular Structure and Function*. Springer-Verlag, New York, Berlin, Heidelberg, Tokyo.
28. V. G. Pivovarenko, A. V. Klueva, A. O. Doroshenko, and A. P. Demchenko (2000) Bands separation in fluorescence spectra of ketocyanine dyes: evidence for their complex formation with monohydric alcohols. *Chem. Phys. Lett.* **325**, 389–398.
29. A. Morimoito, T. Yatsuhashi, T. Shimada, L. Biczok, D. A. Tryk, and H. Inoue (2001) Radiationless Deactivation of an Intramolecular Charge Transfer Excited State through Hydrogen Bonding: Effect of Molecular Structure and Hard-Soft Anionic Character in the Excited State. *J. Phys. Chem. A* **105**, 10488–10496.
30. R. F. Rekker and H. M. de Kort (1979) The hydrophobic fragmental constant. An Extension to a 1000 data point set. *Eur. J. Med. Chem. Chimica Therapeutica* **14**, 479–488.
31. J. M. Mayer, H. van de Waterbeemd, and B. Testa (1982) A comparison between the hydrophobic fragmental methods of Rekker and Leo. *Eur. J. Med. Chem. Chimica Therapeutica* **17**, 17–25.
32. T. Edsall and H. Gutfreund (1983) *Biothermodynamics: The Study of Biochemical Processes at Equilibrium*. John Wiley & Sons, Chichester, New York, Brisbane, Toronro, Singapore.
33. D. Chapman (1975) Phase transitions and fluidity characteristics of lipids and cell membranes. *Q. Rev. Biophys.* **8**, 185–235.
34. R. Koynova and M. Caffrey (1998) Phases and phase transitions of the phosphatidylcholines. *Biochim. Biophys. Acta* **1376**, 91–145.
35. S. P. Verma and D. F. H. Wallah (1976) Multiple thermotropic state transitions in erythrocyte membranes. A laser Raman study of CH-stretching and acoustic regions. *Biochim. Biophys. Acta.* **338**, 121–127.
36. G. Zimmer and H. Schirmer (1974) Viscosity changes of erythrocyte membrane and membrane lipids at transition temperature. *Biochim. Biophys. Acta.* **345**, 314–320.
37. P. R. Cullis (1976) Lateral diffusion rates of PC in vesicules membranes. Effects of cholesterol and hydrocarbon phase transitions. *FEBS Lett.* **68**, 223–228.
38. E. I. Chow, S. Y. Chuang, and P. K. Tseng (1981) Detection of a phase transition in red cell membranes using positronium as a probe. *Biochim. Biophys. Acta* **646**, 356–359.
39. K. Tanaka and D. Ohnishi (1976) Heterogeneity in the fluidity of intact erythrocyte membrane and its homogenization upon hemolysis. *Biochim. Biophys. Acta* **426**, 218–231.
40. N. Pappayee and A. K. Mishra (2000) 1-Naphthol as an excited state proton transfer fluorescent probe for erythrocyte membranes. *Spectrochimica Acta A* **56**, 2249–2253.